JOC The Journal of Organic Chemistry

Article

pubs.acs.org/joc

Site-Specific Description of the Enhanced Recognition Between Electrogenerated Nitrobenzene Anions and Dihomooxacalix[4]arene Bidentate Ureas

Eduardo Martínez-González,[†] Georgina Armendáriz-Vidales,[†] José R. Ascenso,[‡] Paula M. Marcos,*[,§] and Carlos Frontana*[,†]

[†]Centro de Investigación y Desarrollo Tecnológico en Electroquímica, Parque Tecnológico Querétaro Sanfandila, 76703 Sanfandila, Pedro Escobedo, Querétaro, Mexico

[‡]Centro de Química Estrutural, Instituto Superior Técnico, Av. Rovisco Pais, 1049-001 Lisboa, Portugal

[§]Centro de Química Estrutural, Faculdade de Ciências da Universidade de Lisboa, Edifício C8, 1749-016 Lisboa, Portugal

Faculdade de Farmácia da Universidade de Lisboa, Av. Prof. Gama Pinto, 1649-003 Lisboa, Portugal

Supporting Information

ABSTRACT: Electron transfer controlled hydrogen bonding was studied for a series of nitrobenzene derivative radical anions, working as large guest anions, and substituted ureas, including dihomooxacalix[4]arene bidentate urea derivatives, in order to estimate binding constants (K_b) for the hydrogen-bonding process. Results showed enhanced K_b values for the interaction with phenyl-substituted bidentate urea, which is significantly larger than for the remaining compounds, e.g., in the case of 4-methoxynitrobenzene a 28-fold larger K_b value was obtained for the urea bearing a phenyl ($K_b \sim 6888$) vs *tert*-butyl ($K_b \sim 247$) moieties. The respective nucleophilic and electrophilic characters of the participant anion radical and urea hosts were parametrized with global and local electrodonating (ω^-) and electroaccepting (ω^+) powers, derived from DFT calculations. ω^- data were useful for describing trends in structure−activity relationships when comparing nitrobenzene radical anions. However, ω^+ for the host urea structures lead to unreliable explanations of the experimental data. For the latter case, local descriptors $\omega_k^+(r)$ were estimated for the atoms within the urea region in the hosts $[\sum_k \omega_k^+(r)]$. By compiling all the theoretical and experimental data, a K_b-predictive contour plot was built considering ω^- for the studied anion radicals and $\sum_k \omega_k^+(r)$ which affords good estimations.

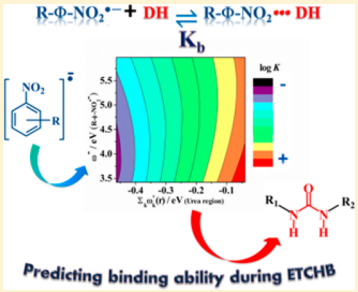

1. INTRODUCTION

Anion recognition by hydrogen-bonding receptors represents a major field of research in supramolecular chemistry, mainly due to the fundamental role played by anions in biology, medicine, and environmental areas. Thus, a large number of macrocyclic compounds have been prepared using hydrogen bond donor groups, such as amides, ureas, and thioureas, to bind anions. These groups provide effective and directional hydrogen bonds.[1−3]

Four decades after the beginning of modern calixarene chemistry, these compounds represent one of the most important classes of macrocycles, mainly in host−guest and supramolecular chemistry.[4] Their availability and easy functionalization at either upper and lower rims afford a large variety of derivatives, which are attractive building blocks for creating host systems of increasing complexity, able to selectively recognize ion and neutral species. In recent years, great effort has been made in the development of calixarene-based anion receptors.[5,6] Calix[4]arenes bearing one or more (thio)urea groups on either the lower or the upper rim have been the most studied for anion recognition.[7−11] Ureidocalix[5]arene[12] and calix[6]arene[13] derivatives have also been tested as anion receptors. Along with calixarene's development, dihomooxacalix[4]arenes (calix[4]arene analogues in which one CH_2 bridge is replaced by one CH_2OCH_2 group),[14] have also been investigated. These macrocycles possess an intermediate size between those of calix[4] and [5]arenes. In recent work,[15,16] the binding abilities of dihomooxacalix[4]arene bidentate urea derivatives showed a dependence on both basicity and geometrical features of anions. Also, as expected due to the higher acidity of their NH groups, arylureas showed higher K_b values compared with alkylureas. Moreover, it is important to notice that binding abilities are dependent on the nature of the substituent groups in each calixarene derivative, and both anion size and shape are crucial for improved binding.

In this context, dihomooxacalix[4]arene derivatives have the potential capacity to host large anions. However, these types of anions are more affected by solvation due to their lower charge-to-radius ratio, resulting in less effective electrostatic interactions and, consequently, limiting their interaction with the intended hosts. While the variety of large anions available

Received: February 25, 2015
Published: April 3, 2015

DOI: 10.1021/acs.joc.5b00441
J. Org. Chem. 2015, 80, 4581−4589

for performing a proper comparison is limited, they can be generated in situ by physicochemical methods. For example, during electron transfer controlled hydrogen bonding (ETCHB),[17−20] radical anions are electrochemically generated and their binding abilities are analyzed by measuring changes in the experimental voltammetric response. This approach has proven useful for comparing binding abilities between structurally different anions.[17−20]

Knowledge of the molecular features of the receptors has been the focus. For example, Gale and co-workers[21] have reported that the acidity of the NH group of some monothioureas directs the anion recognition and mathematical models could predict the transmembrane transport ability. Concerning the anion properties, the partial charge of the atoms involved in the binding process is referred as the most significant factor.[22] Therefore, it becomes necessary to address the influence of particular properties for both host and guest structures, in order to systematically describe the strength of anion binding. For this purpose, reactivity indexes derived from density functional theory (DFT) have been used for evaluating such effects at global and local scales,[23,24] based on the concept of electrophilicity, expressed by[25,26]

$$\omega \equiv \mu^2/2\eta \tag{1}$$

where μ is the chemical potential, and η is the chemical hardness. This definition allows the estimation of the propensity for charge donation or acceptance and is therefore of use to address the nucleophilic or electrophilic character of chemical species, namely the radical anion and the urea-receptor, respectively.[27] For this purpose, two new properties can be calculated, electrodonating (ω^-) and electroaccepting powers (ω^+).[27] While these global reactivity indices, independent of the position of the reactive sites within a molecule, describe the overall scheme, local criteria, $\omega^{\pm}(r)$, provide information within particular regions in the molecules under study. This site-specific analysis could be useful for comparing calix[4]arene derivatives, as previous results have shown that ω^- from electrogenerated anions is proportionally related to K_b values.[17]

In this work, ETCHB between dihomooxacalix[4]arene bidentate urea derivatives and electrogenerated radical anions (substituted nitro- and dinitrobenzenes in their reduced form) is presented (Schemes 1 and 2). Substituent effects on

Scheme 1. Chemical Structures of the Nitrobenzene Derivatives Studied

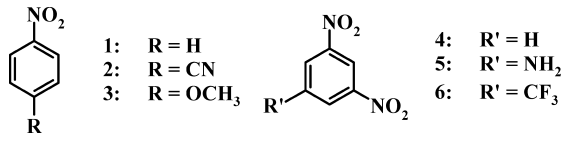

experimental K_b values are discussed in terms of global and local electroaccepting and electrodonating powers, related to each reactive species (anion radical and urea) during the process.

2. RESULTS AND DISCUSSION

2.1. Electrochemical Analysis of Anion Recognition. As referred above, it is important to analyze the effect of large anion recognition by the dihomooxacalix[4]arene bidentate urea compounds being studied (**9** and **10**), which act as

Scheme 2. Chemical Structures of the Urea Derivatives Studied

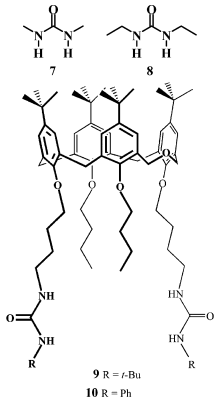

hydrogen bond donor species. For this purpose, ETCHB processes with anion radicals electrogenerated from different nitrobenzene-containing molecules (**1**−**6**) were studied; also, two other model urea compounds (**7** and **8**), were used as comparison. The experimental system can be represented considering the interaction between substituted anion radicals electrogenerated from aromatic nitro compounds (R−ϕ−$NO_2^{\bullet -}$) and hydrogen bond donor species (DH, in this case the studied urea containing compounds) as follows,[17,19]

$$R - \phi - NO_2 + e^- \rightleftharpoons R - \phi - NO_2^- \quad E_{1/2} \tag{2}$$

$$R - \phi - NO_2^- + DH \rightleftharpoons [R - \phi - NO_2^- \cdots DH] \quad K_b \tag{3}$$

Typical voltammetric responses were acquired in experiments performed under different additions of urea derivatives:[17] the reversible electron uptake to generate the radical anion of the nitrocompound (eq 2) begins to shift toward less negative potential values upon increasing the urea concentration in solution by effect of the binding process (eq 3). Due to the mild shifts observed for experiments considering urea compounds **7** and **8**, only data for compounds **9** and **10** are presented in Figure 1, while the rest are shown in the Supporting Information.

Two main effects can be observed: (1) shifts in potential are larger for electron-donating-substituted nitrobenzene (**3**), and (2) shifts are also larger upon interaction with the phenyl-containing dihomooxacalix[4]arene bidentate urea derivative (**10**). For determining K_b values, the experimental variations of $E_{1/2}$ ([DH]) can be fitted using the next equation, proposed by Gómez and co-workers for ETCHB processes[28,29]

$$E_{1/2}([DH]) = E^{0'} + \left(\frac{RT}{F}\right)\ln(1 + K_b[DH]) \tag{4}$$

where $E_{1/2}$([DH]) represents the half-wave DH-concentration-dependent potential, $E^{0'}$ the formal potential of the redox pair, and K_b the binding constant between the radical anion (R−ϕ−$NO_2^{\bullet -}$) and the urea-receptor (DH). Equation 4 considers a 1:1 association which has been previously reported by Marcos for anion recognition between dihomooxacalix[4]arene ureas and anions of different geometry and shape[15] and can be fitted by nonlinear regression with the experimental data (Figure 2). The obtained K_b values are presented in Table 1 and a significantly larger K_b value was determined by the phenyl urea (**10**), compared with the other ureas employed.

DOI: 10.1021/acs.joc.5b00441
J. Org. Chem. 2015, 80, 4581−4589

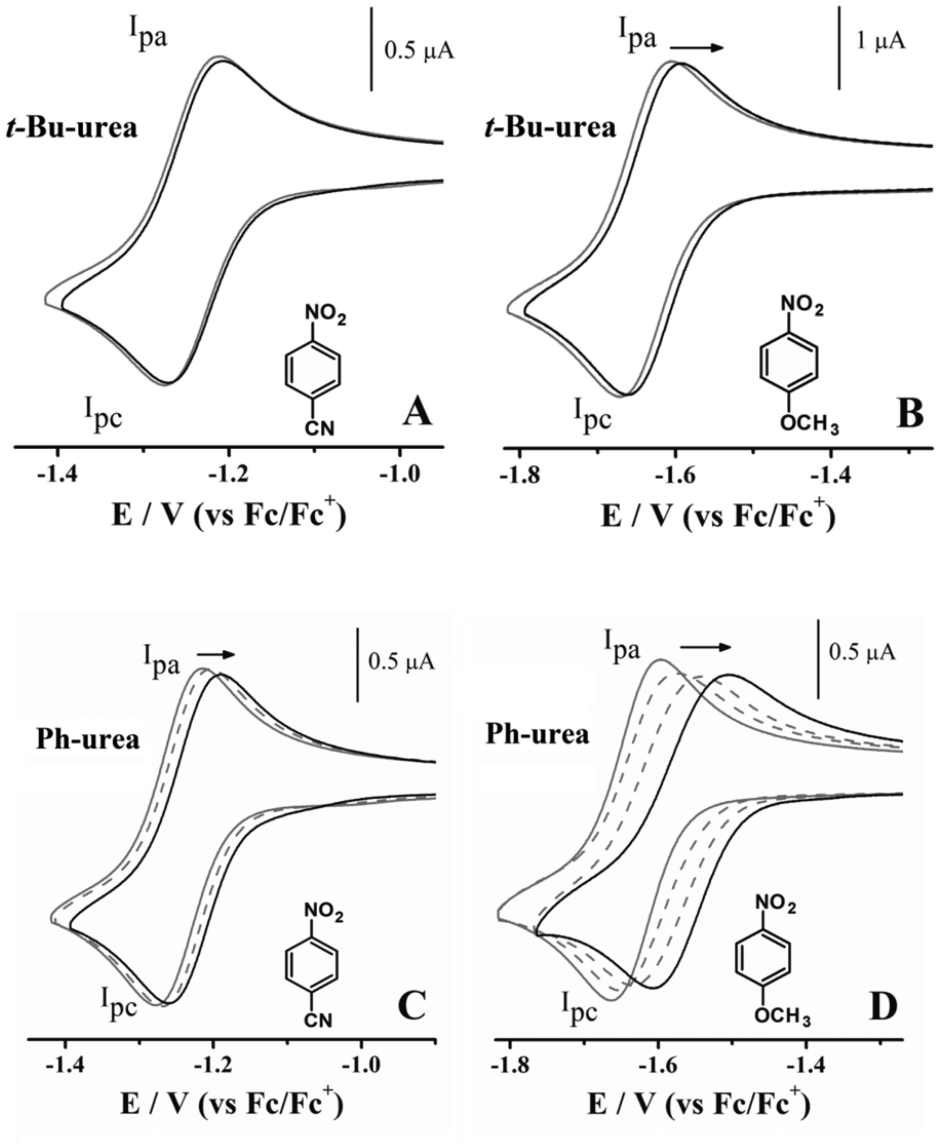

Figure 1. Cyclic voltammograms for (A and C) 4-nitrobenzonitrile (**2**, 0.0004 mol L^{-1}) and (B and D) 4-methoxynitrobenzene (**3**, 0.0009 mol L^{-1}) in CH_3CN/0.1 mol L^{-1} *n*-Bu_4NPF_6, ν = 0.1 V s^{-1}, WE: GC (0.0079 cm^2), with different amounts of added bidentate ureas **9** (A and B) and **10** (C and D), as hydrogen bond donor species (DH): solid gray lines, [DH] = 0 mol L^{-1}, and solid black lines, [DH] = 0.0023 mol L^{-1}. Dashed lines show voltammograms obtained with intermediate DH concentrations. Arrow indicates the direction of shift of the voltammetric signals.

Experimental responses for the interaction between the urea-containing compounds and the electrogenerated anion radicals for **4**−**6** showed also reversible voltammograms, shifted toward less negative potential values upon increasing the urea concentration (Figure 3), as in the above presented case for monosubstituted nitrocompounds **1**−**3** (Figure 1). Again, K_b values were obtained by fitting the observed shifts in $E_{1/2}$ [(DH)] data using eq 4 (Figure 4), and the results are presented also in Table 1.

As occurred for the previously described cases of ETCHB for compounds **1**−**3**, experimental results show that the increase in K_b values relates with the presence of electron-donating groups in the nitro compound structure and are also significantly larger in experiments performed with the studied urea containing a phenyl group (**10**). In particular, compound **10** shows a much higher affinity for all the nitro compounds studied compared with the other urea-containing hosts (**7**−**9**, Table 1). Similar variations in the binding properties for this compound have been previously reported,[15] independently of the geometry of the anion being hosted (either spherical, linear, trigonal planar, or tetrahedral). In order to rationalize the experimental results, it became necessary to employ theoretical reactivity indexes, as this strategy can provide an assessment of the influence of the specific structures for the studied nitro compounds and also of the urea-containing hosts.

2.2. Employment of Global and Local Reactivity Descriptors to Describe Substituent Effects During ETCHB between Electrogenerated Nitrobenzene Anion Radicals and Urea Compounds. With the aim of assessing the observed experimental effects, theoretical descriptors were employed for the studied electrogenerated nitroaromatic radical anions and urea compounds. Due to the nature of the undergoing reaction (eq 3), it is expected that the binding strength is determined by both the nucleophilic and electrophilic characters for the guest anions and urea hosts, respectively. These last properties can be estimated by

DOI: 10.1021/acs.joc.5b00441
J. Org. Chem. 2015, 80, 4581−4589

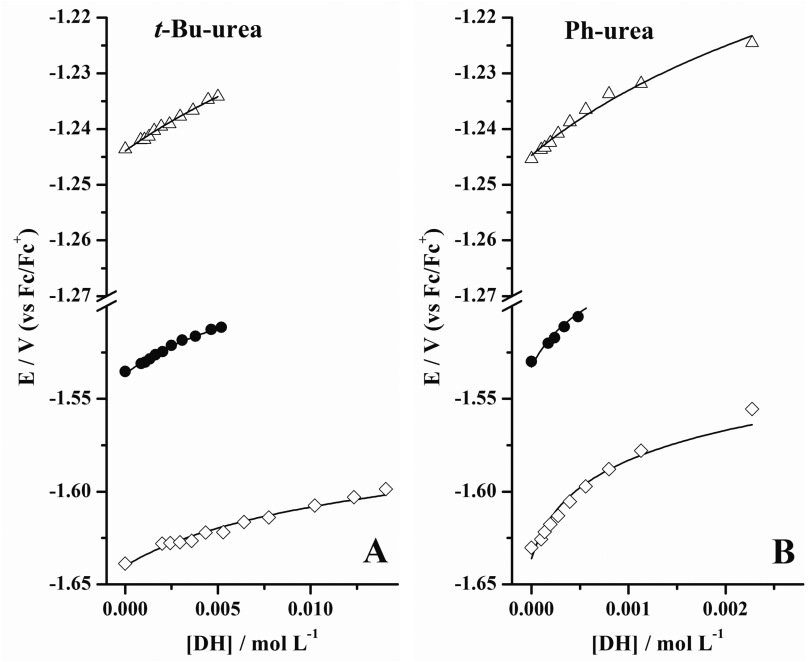

Figure 2. Variations of $E_{1/2}([DH])$ values as a function of added dihomooxacalix[4]arene bidentate urea ([DH]) substituted with (A) *t*-Bu (**9**) and (B) Ph (**10**) for 0.0004 mol L^{-1} (•, **1**) nitrobenzene, (Δ, **2**) 4-nitrobenzonitrile, and (◇, **3**) 4-methoxynitrobenzene. Solid lines represent the fit of the experimental values with equation $E_{1/2}([DH]) = E^{0\prime} + [(RT)/F]\ln(1 + K_b[DH])$.

Table 1. Binding Constants (K_b) for Anion Recognition between Electrogenerated Radical Anions with the Studied Urea Compounds (7−10)

	nitrobenzene compound studied					
urea	**1**	**2**	**3**	**4**	**5**	**6**
7	141 ± 6	28 ± 1	264 ± 27	NA	NA	NA
8	120 ± 7[a]	21 ± 1[a]	172 ± 14[a]	39 ± 1.5	53 ± 1.6	16 ± 0.6
9	322 ± 17.8	92 ± 3	247 ± 25	73 ± 4	156 ± 13	62 ± 3
10	4294 ± 392	575 ± 37	6888 ± 972	2009 ± 170	2162 ± 112	357 ± 26

[a]Data obtained from ref 17. NA: not acquired.

theoretical calculations as they can be derived from the concept of electrophilicity, ω (eq 1), which has led to the construction of reactivity scales for a series of compounds.[24,30]

Within the framework of the DFT, ω is derived from a finite difference approximation to the energy changes in a system[25,26] and becomes[27]

$$\omega \approx \frac{(I + A)^2}{8(I - A)} \tag{5}$$

For addressing the nucleophilic or electrophilic character of a given molecule, two new properties can be calculated, referred as electrodonating (ω^-) and electroaccepting powers (ω^+), respectively,[27]

$$\omega^- \approx \frac{(3I + A)^2}{16(I - A)} \tag{6}$$

$$\omega^+ \approx \frac{(I + 3A)^2}{16(I - A)} \tag{7}$$

Reactivity trends estimated by means of these latter descriptors should consider that, in the case of ω^-, the charge donating process destabilizes the system so that smaller values imply a larger capability to donate electrons. For ω^+, the situation is opposite, as larger values imply an enhanced capacity to accept electrons.[31] Therefore, it is expected that ω^- acts as an index of reactive modulation for the electrogenerated anions[17] and ω^+ would become useful for analyzing the urea-containing counterparts. Minimum energy structures were obtained for the compounds presented in Schemes 1 and 2. However, it is noteworthy that in the case of compounds **9** and **10**, only urea-containing residues were considered (Scheme 3), as they provide the specific anion-binding site of the dihomooxacalix[4]arene compounds under study as has been referred in previous work.[15] Theoretical estimates are presented in Tables 2 and 3.

For identifying trends in behavior, analyses are presented separately for the nitroaromatic radical anions and the urea containing compounds. For the first group (nitro radical anions), ω^- estimations are inversely proportional to the experimental K_b values (Table 1); this tendency was expected, and it is exemplified using experimental data for the binding with urea compounds **9** and **10** plotted in Figure 5, showing that higher values of ω^- refer to lower capacity of the structures to behave as nucleophiles.[17]

On the other hand, for the electrophilic urea structures (Schemes 2 and 3), calculated ω^+ data do not explain the large changes in experimental K_b values (e.g., theoretical estimates for compound **7** are almost similar to those for residue **10**), which is inconsistent with the 28-fold difference in K_b values

DOI: 10.1021/acs.joc.5b00441
J. Org. Chem. 2015, 80, 4581−4589

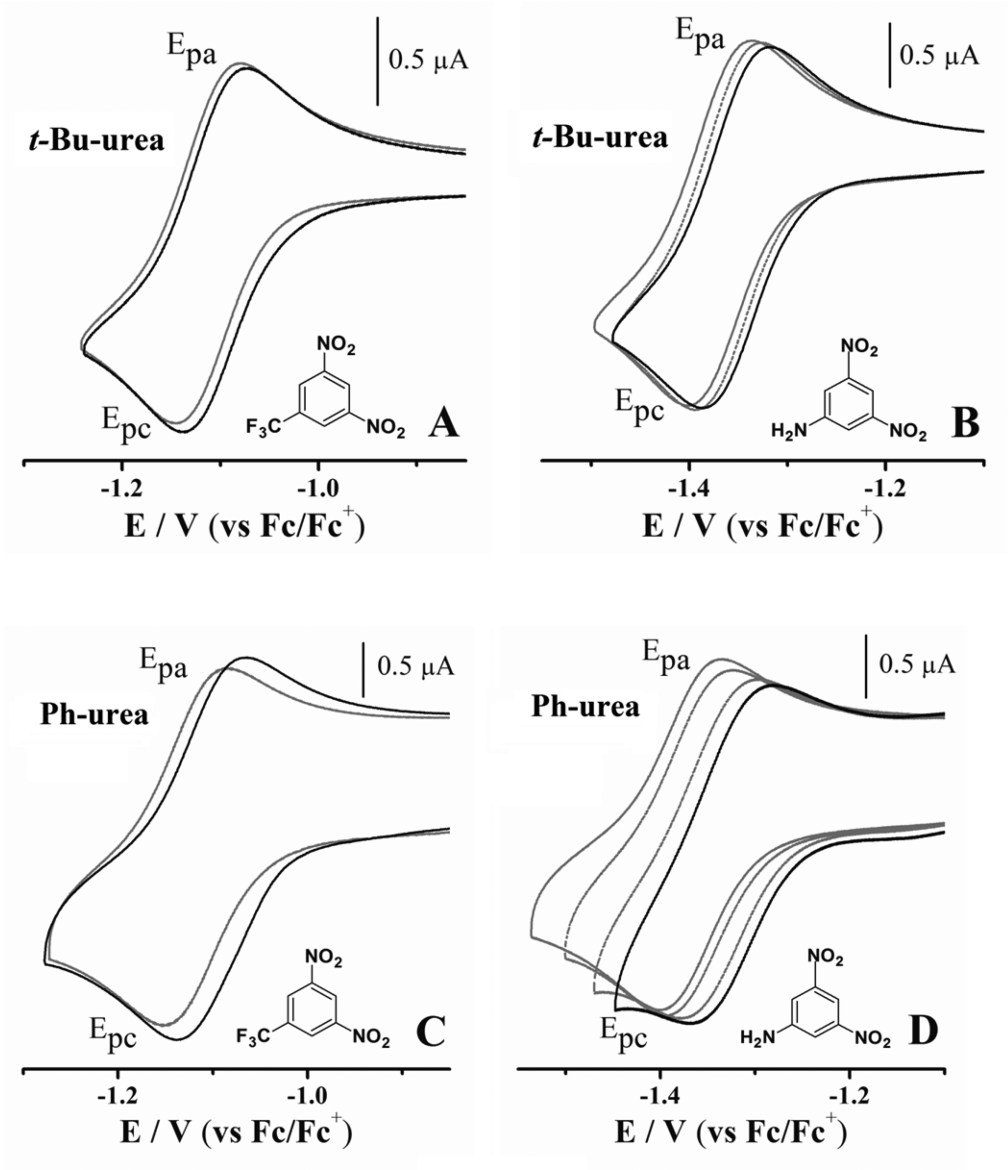

Figure 3. Cyclic voltammograms for 0.0004 mol L^{-1} (A and C) 3,5-dinitrobenzotrifluoride (**6**) and (B and D) 3,5-dinitroaniline (**5**) in CH_3CN/0.1 mol L^{-1} n-Bu_4NPF_6, v = 0.1 V s^{-1}, WE: GC (0.0079 cm^2), with different amounts of added ureas **9** (A and B) and **10** (C and D), as hydrogen bond donor species: solid gray lines, [DH] = 0 mol L^{-1}, and solid black lines, [DH] = 0.0025 mol L^{-1}. Dashed lines show voltammograms obtained with intermediate DH concentrations. Arrow indicates the direction of shift of the voltammetric signals.

upon binding compound **3**. As mentioned before, the acidity of the NH groups is determinant for understanding the anion binding. By this reasoning, site-specific analysis was performed, based on estimation of local electroaccepting power $\omega^+(\boldsymbol{r})$,

$$\omega^+(\mathbf{r}) = \omega^+ f^+[\rho_0, \mathbf{r}] \tag{8}$$

where $f^+[\rho_0, \boldsymbol{r}]$ is the condensed-to-atom variant of the Fukui function related to electron uptake (positive sign);[32,33] using the finite differences approximation, this latter quantity becomes

$$f^+[\rho_0, \mathbf{r}] \approx \rho_{N+1}(\mathbf{r}) - \rho_N(\mathbf{r}) \tag{9}$$

where $\rho_{N+1}(\boldsymbol{r})$ and $\rho_N(\boldsymbol{r})$ are the electronic densities of the system with N + 1 and N electrons at the ground state geometry of the N electron system, respectively. To obtain information about $f^+[\rho_0, \boldsymbol{r}]$, their values can be condensed around each atomic site into a single value that characterizes the atom in the molecule.[34] Therefore, the electronic density differences are calculated by variations in charges around each k^{th} atom, between the N + 1 and N-electron structures, and $f^+[\rho_0, \boldsymbol{r}]$ becomes, by finite differences,

$$f^+[\rho_0, \mathbf{r}] = f_k^+ = q_k(N+1) - q_k(N) \tag{10}$$

$q_k(N + 1)$ and $q_k(N)$ are the charges at the k^{th} atom of the molecule. These values were obtained from a Hirshfeld population analysis, rather than determining its values as a function of the position in space through electronic density differences. This strategy has previously led to consistent values and to predict site reactive effects in agreement with experiments.[35−37] Only selected values associated with the urea moieties were used because, as mentioned above, this region is the reactive site for the binding process (Table 4). For the remaining values, see the Supporting Information.

DOI: 10.1021/acs.joc.5b00441
J. Org. Chem. 2015, 80, 4581−4589

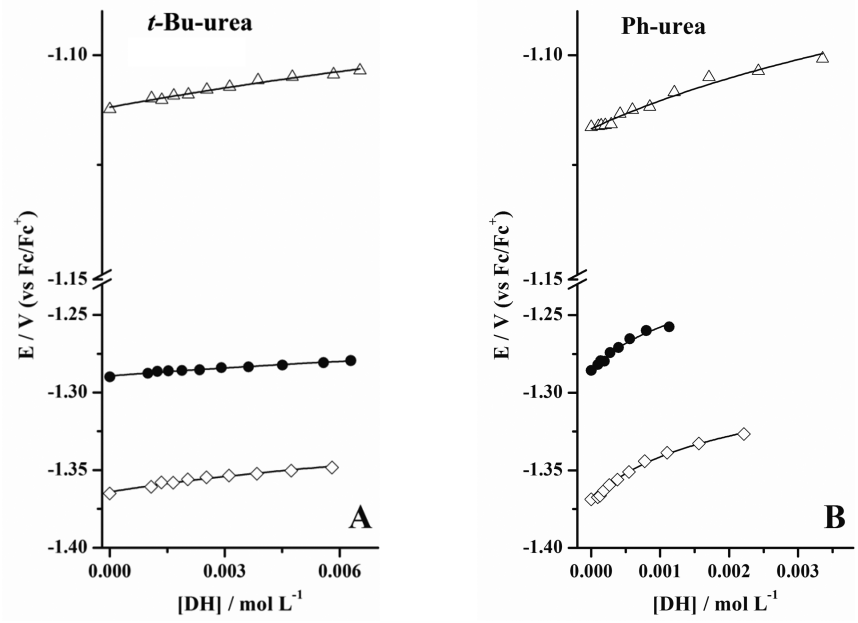

Figure 4. Variations of $E_{1/2}([DH])$ values as a function of added bidentate urea ([DH]) substituted with (**A**) *t*-Bu (**9**) and (**B**) Ph (**10**) for 0.0004 mol L^{-1} (•, **4**) 1,3-dinitrobenzene, (Δ, **6**) 3,5-dinitrobenzotrifluoride, and (◇, **5**) 3,5-dinitroaniline. Solid lines represent the fit of the experimental values with the equation $E_{1/2}([DH]) = E^{0\prime} + [(RT)/F]\ln(1 + K_b[DH])$.

Scheme 3. Structure of the Urea-Containing Residues for Theoretical Calculations, Based on Compounds 9 and 10

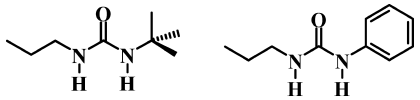

9 10

Table 2. Calculated Vertical Ionization Potentials (I), Vertical Electron Affinities (A), Electrodonating Powers ω^- for the Radical Anion of the Studied Nitro Compounds 1−6

	calculated property (eV)		
compound	I	A	ω^-
1	3.5189	1.1997	3.7246
2	3.8393	1.8950	5.7830
3	3.4621	1.0662	3.4214
4	3.4045	1.8760	5.9762
5	3.3855	1.8710	5.9699
6	3.6225	2.0624	6.6974

Table 3. Calculated Vertical Ionization Potentials (*I*), Vertical Electron Affinities (*A*), Electroaccepting Powers ω^+ for the Studied Urea Compounds

	calculated property (eV)		
compound	I	A	ω^+
7	6.4585	0.4466	0.6322
8	6.4415	0.3951	0.6013
9*	6.4632	0.3573	0.5812
10*	5.7855	0.5540	0.6626

*Calculations were performed for urea-containing residues, see Scheme 3.

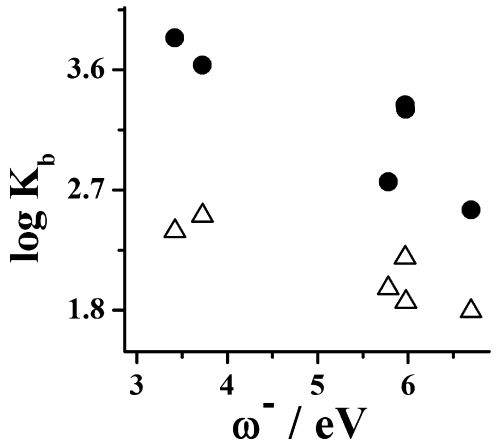

Figure 5. Correlation between calculated ω^- for electrogenerated anion radicals from compounds **1**−**6** and K_b values for urea compounds: (Δ) K_b data from urea-containing residue **9**; (•) K_b data from urea-containing residue **10**.

Table 4. Calculated Charges from Hirshfeld Population Analysis for *N* + 1 and *N*-Electron Structures and Local Electroaccepting Powers $\omega^+(r)$ for the Urea-Containing Compounds 7−10

	calculated property (eV)		
compound	$\sum_k q_k(N+1)$	$\sum_k q_k(N)$	$\sum_k \omega_k^+(r)$
7	−0.9229	−0.1897	−0.4636
8	−0.8480	−0.1756	−0.4043
9[a]	−0.7273	−0.1599	−0.3298
10[a]	−0.14067	−0.0811	−0.0395

[a]Calculations were performed for urea-containing residues (see Scheme 3).

The results showed that the highest value corresponds to the $\sum_k \omega_k^+(r)$ for the fragment containing the phenyl residue (**10**), which suggests that this site is the one more prone for charge acceptance during the hydrogen-bonding process compared to the other ureas. Furthermore, the calculated data for this residue is significantly different from those for compounds **7**−**9**,

DOI: 10.1021/acs.joc.5b00441
J. Org. Chem. 2015, 80, 4581−4589

opposite to the previously described behavior of the global criteria ω^+ (Table 3).

As a summary, the described analysis reveals that comparisons between experimental K_b data with calculated ω^- values of the guest nitroaromatic radical anions and $\sum_k \omega_k^+(r)$ for the host urea region leads to correlations with physical meaning, based on the relative nucleophilic and electrophilic properties of the molecules under study. With the purpose of comparing simultaneously the descriptive character of both criteria, a contour plot (shown in Figure 6) was built by compiling the whole data set obtained from Tables 1, 2, and 4.

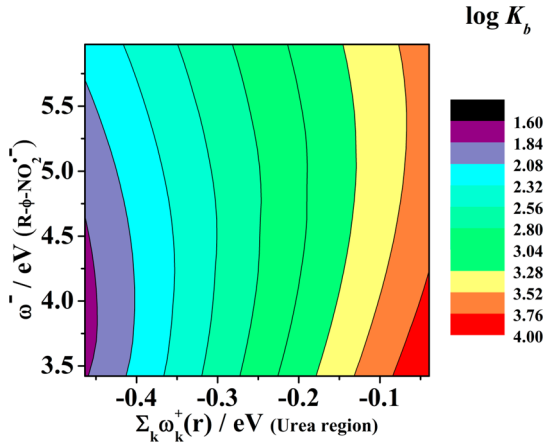

Figure 6. Contour plot of the experimental log K_b values as a function of both ω^- of the radical anion generated from the studied nitrocompounds and $\Sigma_k\omega^+_k(\mathbf{r})$ of the binding site region for the urea-containing host.

The plot presented in Figure 6 allows predicting K_b values for the anion binding process (eq 3) if both ω^- for a given nitroaromatic anion and $\sum_k \omega_k^+(r)$ for a urea-containing residue are estimated. For example, considering data from guest **1** (having a ω^- = 3.7246 eV) and calculated values of $\sum_k \omega_k^+(r)$ for each of the studied urea fragments (Table 4), log K_b values can be estimated as 1.60−1.84, 2.08−2.32, 2.32−2.56, and 3.76−4.00 for host compounds **7**, **8**, **9**, and **10**, respectively. The corresponding experimental values are 2.15, 2.08, 2.51, and 3.63, presenting a fair correlation. It should be noticed that experimental uncertainties become more significant at the bottom left corner of the plot in Figure 6, as this region comprises systems which have low values of K_b, more susceptible to experimental error. Despite this, employment of site-specific criteria (at the global scale for the studied anion radicals and at local sites for the urea hosts) fairly describes the experimental results. It is noteworthy that this approach can only lead to estimates and not exact values, due to the available number of data at the moment which is expected to improve as soon as more information on ETCHB bonding is obtained. Also, other type of host−guest systems could be analyzed as long as the corresponding electrodonating and electroaccepting criteria are identified and specifically estimated for the region involving the binding, regardless of their charge state.

3. CONCLUSIONS

Electron transfer controlled hydrogen bonding was studied for a series of nitrobenzene derivative radical anions, working as large guest anions, and substituted ureas, including dihomooxacalix[4]arene bidentate urea derivatives, in order to estimate binding constants (K_b) for the hydrogen bonding process. Results showed enhanced K_b values for the interaction with phenyl-substituted dihomooxacalix[4]arene bidentate urea, which is significantly larger than for the remaining compounds. The respective nucleophilic and electrophilic characters of the participant anion radical and urea hosts were parametrized with global and local electrodonating (ω^-) and electroaccepting (ω^+) powers, derived from DFT calculations. ω^- Data were useful for describing trends in structure−activity relationships when comparing nitrobenzene radical anions. However, ω^+ for the host urea structures lead to unreliable explanations of the experimental data. For the latter case, local descriptors $\omega_k^+(r)$ were estimated from partial charges $q_k(r)$ of the atoms within the urea region in the hosts $\sum_k \omega_k^+(r)$. By compiling the whole set of theoretical and experimental data, a K_b-predictive contour plot was built considering ω^- for the studied anion radicals and $\sum_k \omega_k^+(r)$, which affords good estimations. This analysis allowed rationalizing the enhanced binding ability of the phenyl-urea compound compared to the other hosts. It was also possible to establish the binding capacities of dihomooxacalix[4]arene bidentate ureas for large anions, in situ electrogenerated.

4. EXPERIMENTAL SECTION

4.1. Chemicals. Electrochemical studies were carried out using 0.0004 and 0.001 mol L^{-1} solutions of nitrobenzene (**1**), 4-nitrobenzonitrile (**2**), 4-methoxy-nitrobenzene (**3**), 1,3-dinitrobenzene (**4**), 3,5-dinitroaniline (**5**), and 3,5-dinitrobenzotrifuoride (**6**) (A.R. grade, without further purification, Scheme 1) dissolved in acetonitrile (extra dry over molecular sieve); these solutions contained 0.1 mol L^{-1} tetrabutylammonium hexafluorophosphate (n-Bu_4NPF_6, dried the night before use at 105 °C) as the supporting electrolyte. All the solutions were maintained under an inert atmosphere by saturation with high-purity nitrogen (grade 5.0) at room temperature (approximately 20 °C). 0.5 mol L^{-1} of 1,3-dimethylurea (**7**) and 1,3-diethylurea (**8**) solutions were prepared in 0.1 mol L^{-1} n-Bu_4NPF_6/CH_3CN with 0.001 mol L^{-1} of the corresponding substituted-nitrobenzenes to avoid dilution during titration experiments. In other experiments, each solution contained 0.007 mol L^{-1} of dihomooxacalix[4]arene bidentate urea derivatives substituted with t-Bu (**9**) and Ph (**10**) residues (Scheme 2), available in previous studies[15] and 0.0004 mol L^{-1} of the other species.

4.2. Instrumentation. Cyclic voltammetry experiments were performed using a potentiostat at a scan rate of ν = 0.1 V s^{-1} and applying IR drop compensation with R_u values determined from positive feedback measurements (R_u = 650 Ω).[38,39] A glassy carbon disk electrode (0.0079 cm^2) was used as the working electrode; the surface was polished with 0.05 μm diamond powder and rinsed successively with acetone and acetonitrile before each voltammetric run. A nonaqueous commercial reference electrode Ag/0.01 mol L^{-1} $AgNO_3$ + 0.1 mol L^{-1} n-Bu_4NClO_4 in acetonitrile and a platinum wire, were used as the reference and auxiliary electrodes, respectively. Potential values obtained are referred to the ferrocene/ferricinium (Fc/Fc^+) couple as recommended by IUPAC.[40]

4.3. Theoretical Section. Geometry optimization and frequency calculations of the chemical structures were performed with the Gaussian 09, revision B.01, using the density functional theory approach and the BHandHLYP functional with a 6-311++G(2d,2p) basis set.[41] Frequency analysis of the structures was carried out after full geometry optimizations, revealing the absence of negative frequencies, thus indicating that the structures are minimum energy conformers. Optimized structures were obtained, considering the solvent effect by the Marenich, Cramer, and Truhlar model.[42] Single point calculations were also performed on the optimized structures in order to determine vertical ionization potential and vertical electron affinity values.

DOI: 10.1021/acs.joc.5b00441
J. Org. Chem. 2015, 80, 4581−4589

■ ASSOCIATED CONTENT

Supporting Information

Chemical structures of the nitrobenzene and urea derivatives studied; cyclic voltammograms for ETCHB experiments for all the compounds with the whole series of studied ureas; nonlinear least-squares fits of experimental $E_{1/2}$ vs Urea Concentration. Internal coordinates as Z-matrices and calculated harmonic frequencies obtained for the minimum energy conformers for the anion radical structure for nitrobenzene derivatives **1**−**6** and neutral structures for urea compounds **7**, **8** and residues associated with molecules **9** and **10** at the BHandHLYP/6-311++G(2d,2p) level considering solvation by the Marenich, Cramer and Truhlar model, Calculated Vertical Ionization Potentials (I), Vertical Electron Affinities (A) for all compounds. Condensed-to-atom q_k values (N+1) and N-electron structures for compounds 7 and 8, and residues 9 and 10; local electroaccepting power $\omega_k^+(r)$ obtained by using the Hirshfeld atomic partitioning scheme. This material is available free of charge via the Internet at http://pubs.acs.org.

■ AUTHOR INFORMATION

Corresponding Authors

*E-mail: pmmarcos@fc.ul.pt. Tel: +351 217500111. Fax: +351 21 7500979.

*E-mail: cfrontana@cideteq mx. Tel: +52 442 2116000, ext 7849. Fax: +52 442 2116001.

Notes

The authors declare no competing financial interest.

■ ACKNOWLEDGMENTS

E.M.-G. and G.A.-V. thank CONACyT-Mexico for support for their Ph.D. studies. C.F. thanks CONACyT-Mexico for support through Project 107037 "Convocatoria SEP-Conacyt Investigación Científica Básica, 2008" and INNOVATEC CONACyT no. 198420, 2013/2014.

■ REFERENCES

(1) Gale, P. A. *Chem. Soc. Rev.* **2010**, *39*, 3746−3771.

(2) Li, A.-F.; Wang, J.-H.; Wang, F.; Jiang, Y.-B. *Chem. Soc. Rev.* **2010**, *39*, 3729−3745.

(3) Bianchi, A.; Bowman-James, K.; García-España, E. In *Anion Coordination Chemistry*; Wiley-VCH: Weinheim, Germany, 2011; pp 1−73.

(4) Gutsche, C. D. *Calixarenes*; Monographs in Supramolecular Chemistry; The Royal Society of Chemistry: Cambridge, 2008; pp P001−P276.

(5) Matthews, S. E.; Beer, P. D. *Supramol. Chem.* **2005**, *17*, 411−435.

(6) Edwards, N. Y.; Possanza, A. L. *Supramol. Chem.* **2013**, *25*, 446−463.

(7) Scheerder, J.; Fochi, M.; Engbersen, J. F. J.; Reinhoudt, D. N. *J. Org. Chem.* **1994**, *59*, 7815−7820.

(8) Babu, J. N.; Bhalla, V.; Kumar, M.; Puri, R. K.; Mahajan, R. K. *New J. Chem.* **2009**, *33*, 675−681.

(9) Modi, N. R.; Patel, B.; Patel, M. B.; Menon, S. K. *Talanta* **2011**, *86*, 121−127.

(10) Stibor, I.; Budka, J.; Michlova, V.; Tkadlecova, M.; Pojarova, M.; Curinova, P.; Lhotak, P. *New J. Chem.* **2008**, *32*, 1597−1607.

(11) Curinova, P.; Stibor, I.; Budka, J.; Sykora, J.; Lang, K.; Lhotak, P. *New J. Chem.* **2009**, *33*, 612−619.

(12) Capici, C.; De Zorzi, R.; Gargiulli, C.; Gattuso, G.; Geremia, S.; Notti, A.; Pappalardo, S.; Parisi, M. F.; Puntoriero, F. *Tetrahedron* **2010**, *66*, 4987−4993.

(13) Hamon, M.; Ménand, M.; Le Gac, S.; Luhmer, M.; Dalla, V.; Jabin, I. *J. Org. Chem.* **2008**, *73*, 7067−7071.

(14) Masci, B. In *Calixarenes*; Asfari, Z., Böhmer, V., Harrowfield, J., Vicens, J., Eds.; Kluwer Academic: Dordrecht, 2001; pp 235−249.

(15) Marcos, P. M.; Teixeira, F. A.; Segurado, M. A. P.; Ascenso, J. R.; Bernardino, R. J.; Michel, S.; Hubscher-Bruder, V. *J. Org. Chem.* **2014**, *79*, 742−751.

(16) Marcos, P. M.; Teixeira, F. A.; Segurado, M. A. P.; Ascenso, J. R.; Bernardino, R. J.; Brancatelli, G.; Geremia, S. *Tetrahedron* **2014**, *70*, 6497−6505.

(17) Martínez-González, E.; Frontana, C. *J. Org. Chem.* **2014**, *79*, 1131−1137.

(18) Smith, D. K. In *Electrochemistry of Functional Supramolecular Systems*; John Wiley & Sons, Inc.: New York, 2009; pp 1−32.

(19) Bu, J.; Lilienthal, N. D.; Woods, J. E.; Nohrden, C. E.; Hoang, K. T.; Truong, D.; Smith, D. K. *J. Am. Chem. Soc.* **2005**, *127*, 6423−6429.

(20) Martinez-Gonzalez, E.; Frontana, C. *Phys. Chem. Chem. Phys.* **2014**, *16*, 8044−8050.

(21) Busschaert, N.; Bradberry, S. J.; Wenzel, M.; Haynes, C. J. E.; Hiscock, J. R.; Kirby, I. L.; Karagiannidis, L. E.; Moore, S. J.; Wells, N. J.; Herniman, J.; Langley, G. J.; Horton, P. N.; Light, M. E.; Marques, I.; Costa, P. J.; Felix, V.; Frey, J. G.; Gale, P. A. *Chem. Sci.* **2013**, *4*, 3036−3045.

(22) Baggi, G.; Boiocchi, M.; Fabbrizzi, L.; Mosca, L. *Chem.−Eur. J.* **2011**, *17*, 9423−9439.

(23) Pérez, P.; Simón-Manso, Y.; Aizman, A.; Fuentealba, P.; Contreras, R. *J. Am. Chem. Soc.* **2000**, *122*, 4756−4762.

(24) Pérez, P.; Domingo, L. R.; Aizman, A.; Contreras, R. In *Theoretical Aspects of Chemical Reactivity*; Torro-Labbé, A., Ed.; Theoretical and Computational Chemistry; Elsevier: Amsterdam, 2007; Vol. *19*, pp 139−201.

(25) Parr, R. G.; Donnelly, R. A.; Levy, M.; Palke, W. E. *J. Chem. Phys.* **1978**, *68*, 3801.

(26) Parr, R. G.; Pearson, R. G. *J. Am. Chem. Soc.* **1983**, *105*, 7512−7516.

(27) Gázquez, J. L.; Cedillo, A.; Vela, A. *J. Phys. Chem. A* **2007**, *111*, 1966−1970.

(28) Gómez, M.; González, F. J.; González, I. *Electroanalysis* **2003**, *15*, 635−645.

(29) Gómez, M.; González, F. J.; González, I. *J. Electrochem. Soc.* **2003**, *150*, E527−E534.

(30) Domingo, L. R.; Aurell, M. J.; Pérez, P.; Contreras, R. *Tetrahedron* **2002**, *58*, 4417−4423.

(31) Gázquez, J. L. *J. Mex. Chem. Soc.* **2008**, *52*, 3−10.

(32) Parr, R. G.; Yang, W. *J. Am. Chem. Soc.* **1984**, *106*, 4049−4050.

(33) Contreras, R. R.; Fuentealba, P.; Galván, M.; Pérez, P. *Chem. Phys. Lett.* **1999**, *304*, 405−413.

(34) Mendez, F.; Gazquez, J. L. *J. Am. Chem. Soc.* **1994**, *116*, 9298−9301.

(35) Parr, R. G.; Yang, W. *Density-Functional Theory of Atoms and Molecules*; International Series of Monographs on Chemistry; Oxford University Press, New York, 1989.

(36) Garza, J.; Vargas, R.; Cedillo, A.; Galván, M.; Chattaraj, P. *Theor. Chem. Acc.* **2006**, *115*, 257−265.

(37) Armendáriz-Vidales, G.; Hernández-Muñoz, L. S.; González, F. J.; de Souza, A. A.; de Abreu, F. C.; Jardim, G. A. M.; da Silva, E. N.; Goulart, M. O. F.; Frontana, C. *J. Org. Chem.* **2014**, *79*, 5201−5208.

(38) Roe, D. K. In *Laboratory Techniques in Electroanalytical Chemistry*, 2nd Ed.; revised and expanded; Kissinger, P., Heineman, W. R., Eds.; Taylor & Francis: Abingdon, Oxon, U.K., 1996.

(39) He, P.; Faulkner, L. R. *Anal. Chem.* **1986**, *58*, 517−523.

(40) Gritzner, G.; Kuta, J. *Pure Appl. Chem.* **1984**, *56*, 461−466.

(41) Frisch, M. J.; Trucks, G. W.; Schlegel, H. B.; Scuseria, G. E.; Robb, M. A.; Cheeseman, J. R. Scalmani, G.; Barone, V.; Mennucci, B.; Petersson, G. A.; Nakatsuji, H.; Caricato, M.; Li, X.; Hratchian, H. P.; Izmaylov, A. F.; Bloino, J.; Zheng, G.; Sonnenberg, J. L.; Hada, M.; Ehara, M.; Toyota, K.; Fukuda, R.; Hasegawa, J.; Ishida, M. .; Nakajima, T.; Honda, Y.; Kitao, O.; Nakai, H.; Vreven, T.; Montgomery, J. A. J.; Peralta, J. E.; Ogliaro, F.; Bearpark, M.; Heyd, J. J.; Brothers, E.; Kudin, K. N.; Staroverov, V. N.; Kobayashi, R.; Normand, J.; Raghavachari, K.; Rendell, A.; Burant, J. C.; Iyengar, S. S.;

DOI: 10.1021/acs.joc.5b00441
J. Org. Chem. 2015, 80, 4581−4589

Tomasi, J.; Cossi, M.; Rega, N.; Millam, J. M.; Klene, M.; Knox, J. E.; Cross, J. B.; Bakken, V.; Adamo, C.; Jaramillo, J.; Gomperts, R.; Stratmann, R. E.; Yazyev, O.; Austin, A. J.; Cammi, R.; Pomelli, C.; Ochterski, J. W.; Martin, R. L.; Morokuma, K.; Zakrzewski, V. G.; Voth, G. A.; Salvador, P.; Dannenberg, J. J.; Dapprich, S.; Daniels, A. D.; Farkas, O.; Foresman, J. B.; Ortiz, J. V.; Cioslowski, J. *Gaussian 09*, revision B.01; Gaussian, Inc.: Wallington, CT, 2010.

(42) Marenich, A. V.; Cramer, C. J.; Truhlar, D. G. *J. Phys. Chem. B* **2009**, *113*, 6378−6396.

DOI: 10.1021/acs.joc.5b00441
J. Org. Chem. 2015, 80, 4581−4589